In vivo anatomy of the Neer and Hawkins sign positions for shoulder impingement

George P. Pappas, MD, PhD,[a] Silvia S. Blemker, PhD,[b] Christopher F. Beaulieu, MD, PhD,[c] Timothy R. McAdams, MD,[d] Sean T. Whalen, BS,[e] and Garry E. Gold, MD,[c] *Stanford, CA*

The Neer and Hawkins impingement signs are commonly used to diagnose subacromial pathology, but the anatomy of these maneuvers has not been well elucidated in vivo. This 3-dimensional open magnetic resonance imaging study characterized shoulder anatomy and rotator cuff impingement in 8 normal volunteers placed in the Neer and Hawkins positions. Subacromial and intraarticular contact of the rotator cuff was graded, and minimum distances were computed between the tendon insertion sites and the glenoid, acromion, and coracoid. Both the Neer and Hawkins maneuvers significantly decreased the distance from the supraspinatus insertion to the acromion and posterior glenoid and from the subscapularis insertion to the anterior glenoid. However, the Hawkins position resulted in significantly greater subacromial space narrowing and subacromial rotator cuff contact than the Neer position. In the Hawkins position, subacromial contact of the supraspinatus and infraspinatus was observed in 7 of 8 and 5 of 8 subjects, respectively. In contrast, rotator cuff contact with the acromion did not occur in any subject in the Neer position. Intraarticular contact of the supraspinatus with the posterosuperior glenoid was observed in all subjects in both positions. Subscapularis contact with the anterior glenoid was also seen in 7 of 8 subjects in the Neer position and in all subjects in the Hawkins position. This extensive intraarticular contact suggests that internal impingement may play a role in the Neer and Hawkins signs. (J Shoulder Elbow Surg 2006;15:40-49.)

From the Stanford University School of Medicine and Departments of Bioengineering, Radiology, Orthopaedics, and Mechanical Engineering, Stanford University.

This research was supported by a Stanford University School of Medicine Medical Scholars research grant to Dr Pappas.

Reprint requests: Garry E. Gold, MD, Stanford University Medical Center, 300 Pasteur Dr, Room S-068, Stanford, CA 94305-5105 (E-mail: *gold@stanford.edu*).

1058-2746/2006/$32.00
doi:10.1016/j.jse.2005.04.007

Impingement syndrome is a common cause of shoulder pain arising from the repetitive or excessive contact of the rotator cuff tendons with other anatomic structures in the shoulder. Shoulder impingement can be classified as either external or internal. First described by Neer[33] in 1972, external impingement is characterized by contact of the superficial aspect of the rotator cuff against the acromion, coracoid process, or coracoacromial ligament. In 1992 internal impingement was described in arthroscopic and cadaveric studies as contact of the undersurface of the supraspinatus and infraspinatus tendons with the posterosuperior glenoid rim or labrum.[27,41] Internal impingement has been proposed as an etiologic mechanism of pathology observed on the articular side of the rotator cuff.

The Neer and Hawkins impingement signs are believed to be reliable indicators of subacromial external impingement.[30,40] To elicit the Neer impingement sign, an examiner passively elevates the patient's shoulder to the position of maximal elevation while stabilizing the scapula.[1] Hawkins and Kennedy[26] proposed a modified maneuver of forward flexion to 90° combined with maximal internal rotation of the shoulder. Shoulder pain elicited in these positions is thought to result from subacromial impingement with rotator cuff pathology.[30] Despite the sensitivity of the Neer and Hawkins signs, their poor specificity and positive predictive value[8,29,30] suggest the existence of additional alternative impingement mechanisms.[35]

The anatomy and impingement mechanisms of these maneuvers have not been well elucidated in vivo.[14] Biomechanical analyses of shoulder abduction and rotation predict that the Hawkins sign position should result in greater subacromial contact of the rotator cuff than the Neer sign position.[6,7,14,23,25,38] However, a recent in vivo study of asymptomatic volunteers did not observe subacromial contact of the rotator cuff in either the Neer or the Hawkins sign position.[35] Furthermore, whereas internal impingement in the Neer and Hawkins positions has been suggested by recent skeletal[12] and cadaveric[40] studies, this mechanism has not been demonstrated in vivo.

The goal of this open magnetic resonance imaging

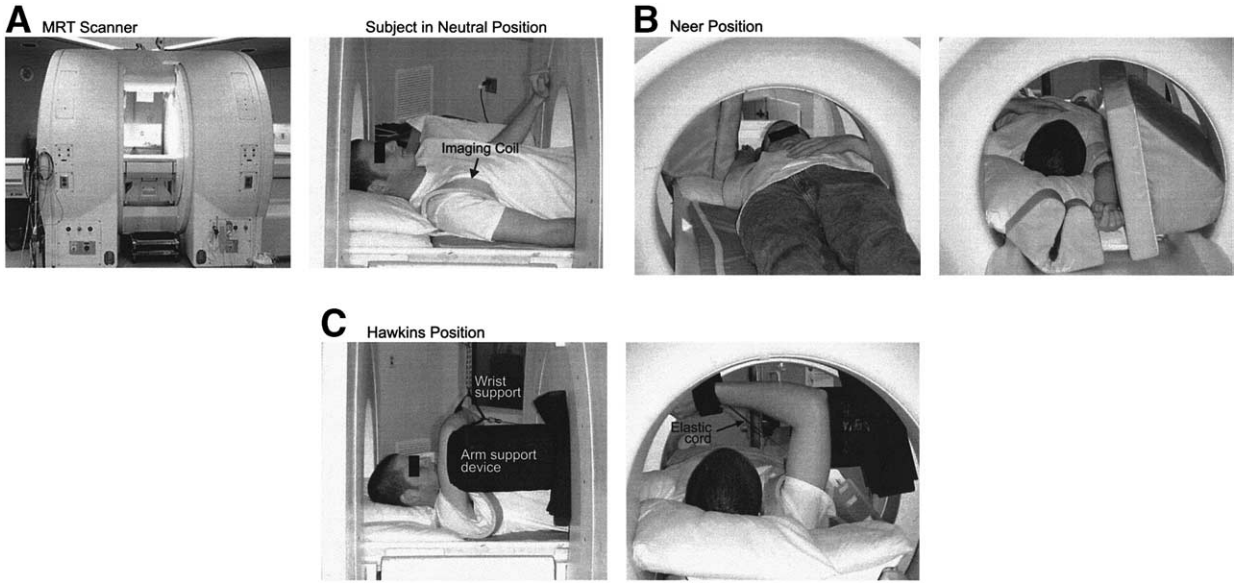

Figure 1 Subject positioning within MR scanner. **A**, The open MRI scanner (MRT, Magnetic Resonance Therapy) used for this study is depicted in the *left panel*. The *right panel* shows a subject supine within the scanner in the neutral position, with his arm at his side. **B**, To simulate the Neer position, the subject's right arm was placed in the overhead position with palm facing up, with the arm being held stationary by foam pads. **C**, To simulate the Hawkins position, the subject's relaxed right arm and wrist were supported at 90° of forward shoulder flexion and 90° of elbow flexion. An internal rotation torque was then applied by use of an elastic cord attached to the wrist band.

(MRI) study was to characterize the in vivo anatomy of the shoulder in the Neer and Hawkins positions. Specifically, we tested the following two hypotheses: (1) the Hawkins position brings the rotator cuff tendon insertion sites into closer proximity of the acromion than the Neer position and (2) the Neer and Hawkins maneuvers elicit internal impingement, as well as external impingement, of the rotator cuff. MRI was used to assess articular contact of the rotator cuff with the glenoid rim and labrum, as well as superficial contact of the rotator cuff in the subacromial space. Three-dimensional (3D) computer models of shoulder anatomy were also generated from the magnetic resonance (MR) images, and minimum distances were computed from the greater tuberosity, lesser tuberosity, and rotator cuff tendon insertion sites of the humerus to the acromion, glenoid rim, and coracoid process of the scapula.

MATERIALS AND METHODS

Eight normal volunteers with no history of shoulder pain or pathology participated in this study. All subjects were men ranging in age from 19 to 21 years. Before MRI, a physical examination of the shoulder was performed on each subject by the same examiner. All subjects exhibited normal surface anatomy, range of motion, strength, and stability; no tenderness to palpation was elicited. The Neer and Hawkins impingement signs were also negative for all subjects. The Institutional Review Board of Stanford University, Stanford, CA, approved the protocol, and informed consent was obtained from each subject.

MRI

MRI was performed with the subject in the supine position in a 0.5-T open MR scanner (Signa SP; GE Medical Systems, Milwaukee, WI). The right shoulder was imaged by use of a flexible, circular radiofrequency surface coil (Figure 1). Images were acquired by use of a 3D gradient-recalled echo (GRE) pulse sequence with 20 milliseconds of echo time, 37 milliseconds of repetition time, a 20 × 20–cm field of view, and a 256 × 160–pixel matrix. Each 3D GRE scan yielded 42 consecutive 2-dimensional images with a slice thickness of 2 mm and required a total scan time of 4 minutes 35 seconds.

Subjects were imaged with the right arm in three different positions: (1) neutral, with the arm resting at the subject's side; (2) the Neer position; and (3) the Hawkins position (Figure 1). First, 3D GRE images of the right shoulder in the neutral position were acquired in both the coronal and axial planes (Figure 2). Subsequently, axial images of the shoulder were acquired with the arm in the Neer and Hawkins examination positions. To image the shoulder in the Neer impingement sign position, the subject's extended right arm was placed in full forward flexion (Figure 1, *B*). For the Hawkins impingement sign position, the right arm was positioned at 90° of forward flexion by use of a plastic arm-supporting device (Figure 1, *C*). In addition, the forearm was supported at the wrist to maintain an elbow flexion angle of 90°, and the shoulder was internally rotated by application of an inferiorly directed

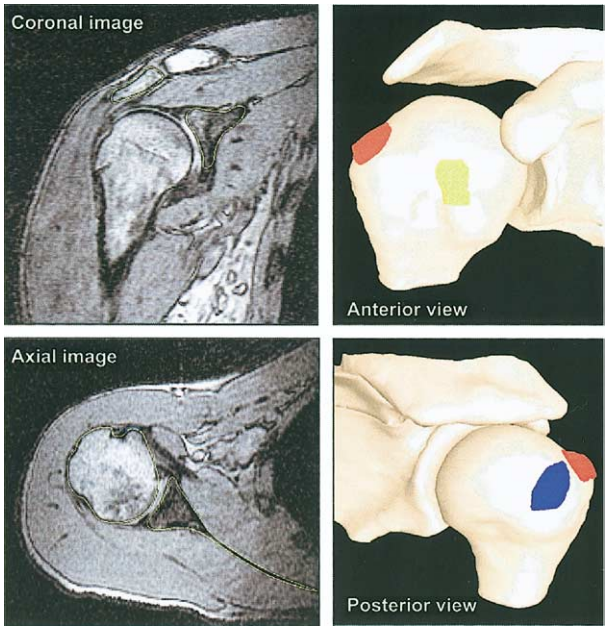

Figure 2 Segmentation of shoulder anatomy from MR images. The boundaries of the bones and muscle attachments were outlined in each image slice, and a 3D surface model for each structure was built from the series of outlines.

force of 9.8 N at the wrist by use of a calibrated elastic cord (Figure 1, *C*). The amount of force applied at the wrist was chosen to simulate the forced internal rotation produced during a clinical examination without causing excessive discomfort during the approximately 5-minute-long scan. Subjects were at rest and did not actively resist the internal rotation imposed by the elastic cord. A goniometer was used to confirm arm orientation in the impingement positions and to measure internal rotation in the Hawkins position, which averaged 111° ± 8° for the 8 subjects. The order in which the subjects were placed in the impingement positions was varied; even-numbered subjects were first imaged in the Neer position and subsequently imaged in the Hawkins position, whereas odd-numbered subjects were placed in the Hawkins position first and then in the Neer position.

Radiologic grading of rotator cuff impingement

Rotator cuff impingement was assessed from the axial MR images of the shoulder in the Neer and Hawkins positions. Internal and external impingement of the supraspinatus, infraspinatus, and subscapularis tendons was characterized by consensus grading of 2 musculoskeletal radiologists. No impingement of the teres minor tendon was seen. Images were reviewed interactively, and multiplanar reformatting was used as needed (Advantage Windows, GE Medical Systems, Milwaukee, WI). For both positions, contact of the supraspinatus and infraspinatus with the acromion and the subscapularis with the coracoid process was assessed; contact with the glenoid-labrum complex was also graded for the three rotator cuff tendons. Impingement was graded based on the extent of rotator contact with the scapula. A grade of 0 was assigned if the rotator cuff did not make contact with the structure; a grade of 1 or 2 was assigned if contact occurred either without (grade 1) or with (grade 2) deformation of the rotator cuff muscle-tendon complex.

Computer modeling

Three-dimensional surface models of the glenoid, coracoid, acromion, labrum, and supraspinatus, infraspinatus, and subscapularis insertion sites were created from each series of contiguous 2-dimensional MR images. In each 2-dimensional image, the anatomic structures were outlined manually by defining a series of points that were connected by a cardinal spline. The outlines for each structure were then combined to form a 3D polygonal surface mesh (Nuages; INRIA Sophia-Antipolis, Sophia-Antipolis, France). The resulting surface models of the anatomic structures were imported into a graphics-based musculoskeletal modeling environment, SIMM (Software for Interactive Musculoskeletal Modeling; Musculographics, Inc, Santa Rosa, CA).[10]

In the Hawkins and Neer positions, surface models for the humerus, glenoid, and acromion were created from the single set of axial images obtained in each position. In the neutral position, surface models for all structures were built from both axial and coronal image series and combined to form a complete representation (Figure 2). For example, the proximal aspect of the humeral head was taken from the coronal reconstruction and added to the axial reconstruction to form a full reconstruction of the proximal humerus. The humerus and scapula from the detailed neutral position models were registered to the humerus and scapula reconstructions in the Hawkins and Neer positions. Performing this registration step allowed the use of the detailed reconstructions generated from the neutral position images—which included optimal coverage of the muscle insertions—to calculate minimum distances in the Hawkins and Neer positions.

An iterative closest-point algorithm[3] and a nonlinear, least squares algorithm (MATLAB Optimization Toolbox; The Mathworks, Natick, MA) were used to register the surface reconstructions of the humerus and scapula in the neutral position to the humerus and scapula models in the Hawkins and Neer positions. The inputs to the algorithm were two polygonal surfaces that were originally at a distance from each other. The algorithm determined the transformation to be applied to one of the surfaces to minimize the distance between the two surfaces. This algorithm has been widely used; for example, it has been used to calculate scapular kinematics[16] and to register lower limb bone surfaces built from orthogonal sets of MR images.[2]

Calculation of minimum distances

Minimum distances between the humerus and the scapula were calculated. Specifically, minimum distances were computed between (1) the greater and lesser tuberosities and supraspinatus, infraspinatus, and subscapularis insertion sites of the humerus and (2) the glenoid, acromion, and coracoid process of the scapula. For each polygon in each humeral surface, the closest point on the scapular surface was found; the minimum distance between the two surfaces was the closest polygon-point distance (Figure 3, *A*). The

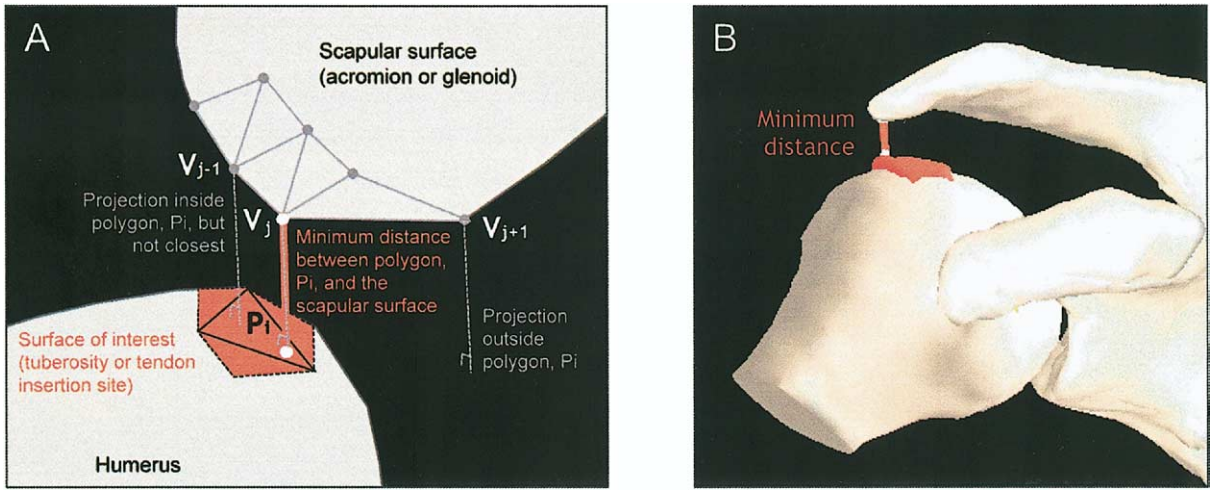

Figure 3 Determination of minimum distances. **A**, For each polygon (*Pi*) on the humeral surface, the closest point (*Vj*) on the scapular surface was found. The closest point was the one that projected onto the plane of the polygon (1) within the boundary of the polygon (note that the projection of Vj+1 is outside the boundary) and (2) the closest (note that the projection of Vj is closer than the projection of Vj-1). The closest polygon-point match was selected as the minimum distance between the two surfaces. **B**, The points of minimum distance were then displayed graphically. For example, the *red surface* on the humerus is the supraspinatus tendon insertion and the *red line* indicates the minimum distance between the insertion and the acromion.

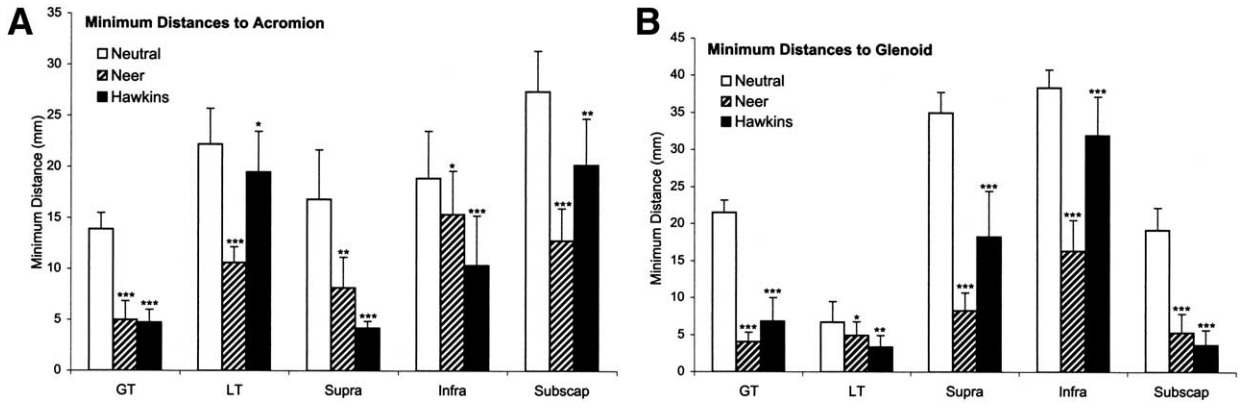

Figure 4 Minimum distances to acromion (**A**) and glenoid (**B**) from greater tuberosity (*GT*), lesser tuberosity (*LT*), and insertions of supraspinatus (*Supra*), infraspinatus (*Infra*), and subscapularis (*Subscap*) tendons. Note that the supraspinatus and infraspinatus insertion minimum distances follow the same trend as the greater tuberosity minimum distance. Similarly, the minimum distances to the subscapularis tendon insertion and the lesser tuberosity follow the same trend. The *bars* represent the mean value for all 8 subjects, and the *error bars* represent 1 SD. In every case the minimum distances computed for the Neer and Hawkins positions were significantly smaller than the corresponding minimum distance in the neutral position. The level of significance is given by the number of asterisks as follows: *1 asterisk*, $P < .05$; *2 asterisks*, $P < .01$; and *3 asterisks*, $P < .001$.

closest points on the two surfaces were displayed graphically (Figure 3, *B*). Minimum distances for the neutral, Neer, and Hawkins positions were compared by use of paired *t* tests. Descriptive statistics are reported as mean values ± SD.

RESULTS

Subacromial impingement

The greater tuberosity was significantly closer to the acromion in both the Neer and Hawkins positions than in the neutral position (Figure 4, *A*). However, the minimum distance from the greater tuberosity to the acromion did not differ significantly between the two impingement sign positions ($P = .78$). The minimum distance from the supraspinatus and infraspinatus tendon insertion sites to the acromion also decreased significantly in the impingement positions compared with the neutral position (Figure 4, *A*). Moreover, the supraspinatus insertion was significantly closer to the acromion than the infraspinatus insertion for

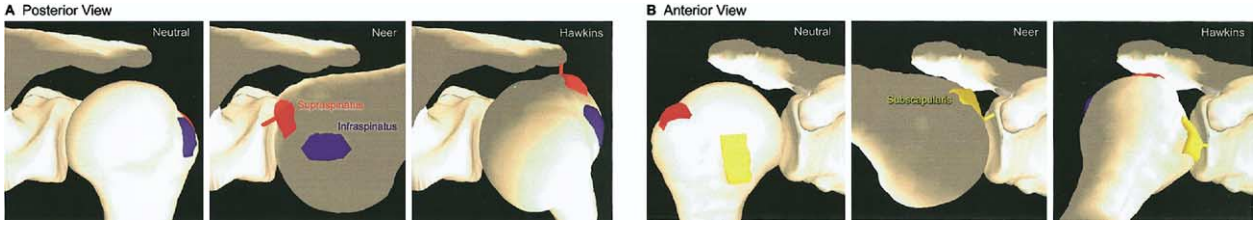

Figure 5 Surface models of shoulder anatomy in neutral, Neer, and Hawkins positions. **A**, The posterior view of the shoulder anatomy in subject 6 demonstrates the proximity of the greater tuberosity and the supraspinatus insertion (*red*) to the glenoid in the Neer position and to the acromion in the Hawkins position. The *red line* is the minimum distance vector from the supraspinatus insertion to the glenoid in the Neer position and to the acromion in the Hawkins position. The infraspinatus insertion site (*blue*) is not in close proximity to the scapula in either impingement position. **B**, The anterior view of the shoulder anatomy in subject 3 depicts the close proximity of the lesser tuberosity and the subscapularis insertion (*yellow*) to the anterior glenoid in both the Neer and Hawkins positions. The minimum distance vector from the subscapularis insertion to the glenoid is shown in *yellow*. Also note the subacromial position of the supraspinatus insertion (*red*) and its close proximity to the distal acromion.

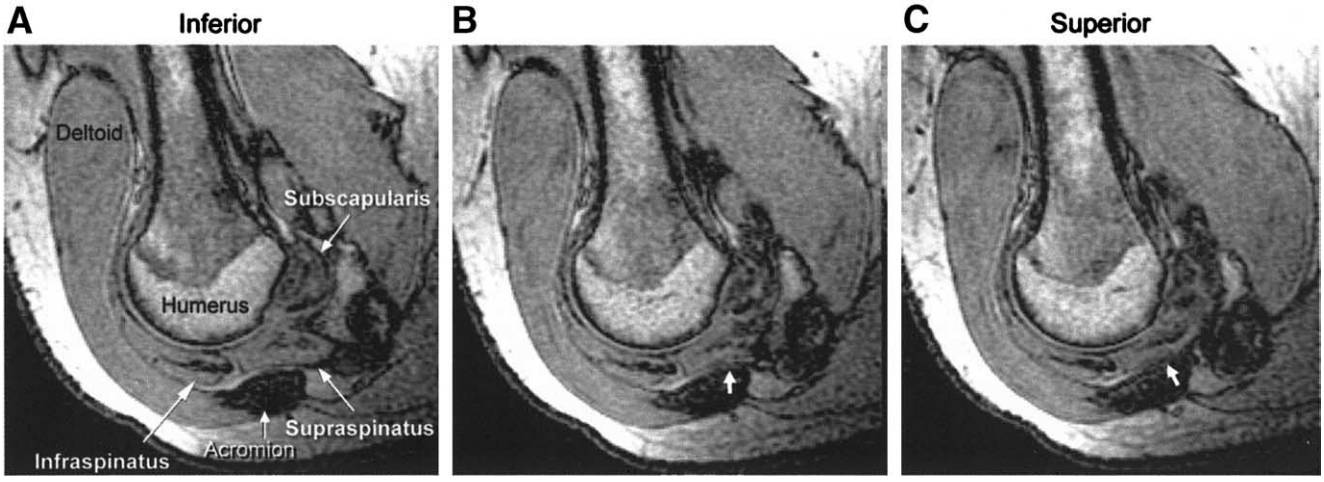

Figure 6 Subacromial impingement. The images are contiguous 2-mm-thick axial slices acquired with subject 6 in the Hawkins position; **A** is inferior to **B**, and **C** is superior to **B**. **A**, The deformation and curvature associated with grade 2 supraspinatus impingement are best appreciated in the most inferior axial image. **B** and **C**, Contact of the supraspinatus with the anteromedial acromion is best seen superiorly (*white arrows*).

both the Neer ($P < .001$) and Hawkins ($P < .01$) positions (Figure 5, *A*). Both insertion sites were significantly ($P < .01$) closer to the acromion in the Hawkins position than in the Neer position. In the Hawkins position, the distance from the supraspinatus insertion to the acromion averaged only 4.2 ± 0.7 mm.

In the Neer position, the radiologic grading results showed that the rotator cuff did not make contact with the underside of the acromion in any subject. The muscular portion of the supraspinatus did make contact with the acromion at its base, near the scapular spine, but not within the subacromial space. The infraspinatus did not make contact with the acromion. In contrast, in the Hawkins position, impingement of the supraspinatus with the medial or anteromedial acromion was seen in 7 of 8 subjects (Figure 6), and infraspinatus contact with the lateral or mid acromion was seen in 5 of 8 subjects.

The lesser tuberosity and subscapularis tendon insertion site were also significantly closer to the acromion in the impingement positions than in the neutral position (Figure 4, *A*). Although the subscapularis insertion was significantly closer ($P < .01$) to the acromion in the Neer position (12.8 ± 3.2 mm) than in the Hawkins position (20.2 ± 4.5 mm), the insertion site was not in close proximity to the acromion in either position. Contact of the subscapularis with the acromion was not observed on the MR images for either impingement position.

Coracoid impingement

The minimum distance between the lesser tuberosity and the coracoid process decreased significantly from 14.3 ± 1.6 mm in the neutral position to $11.2 \pm$

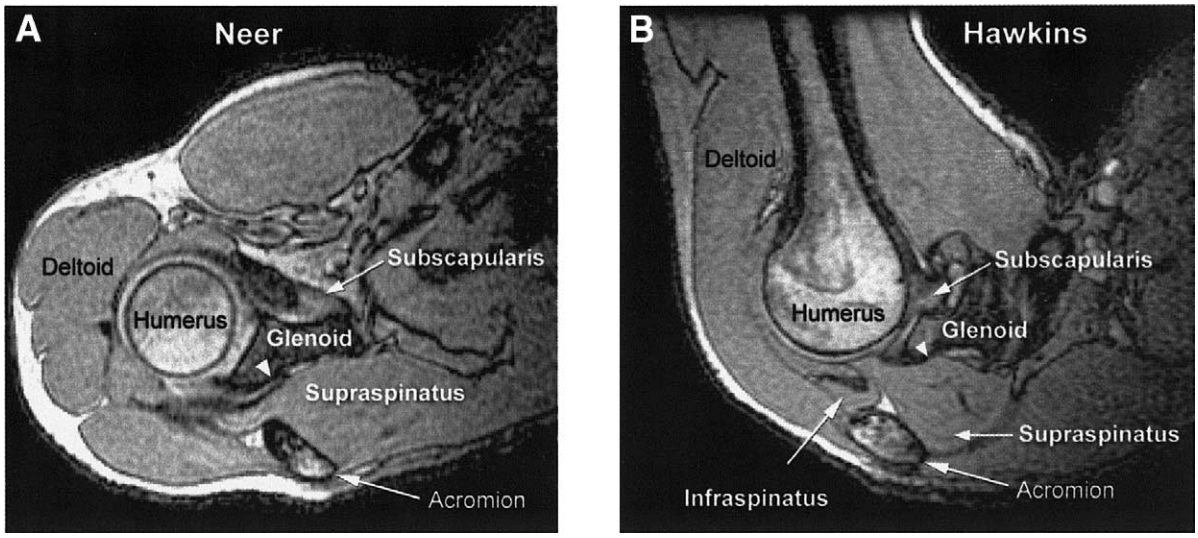

Figure 7 Internal glenoid impingement. Both images were acquired in the axial plane with subject 7 in the Neer position (**A**) and Hawkins position (**B**). In both cases the supraspinatus made contact with the posterosuperior glenoid and produced deformation of the tendon (**A**) or muscle (**B**); an impingement grade of 2 was assigned in each case. Note that the location of impingement was more distal at the tendon in the Neer position (**A**) as compared with impingement of the muscle in the Hawkins position.

2.6 mm in the Neer position ($P < .05$) and 10.9 ± 2.3 mm in the Hawkins position ($P < .01$). Similarly, the distance from the subscapularis insertion to the coracoid decreased significantly from 14.6 ± 1.8 mm in the neutral position to 11.4 ± 2.7 mm in the Neer position ($P < .05$) and 10.2 ± 2.3 mm in the Hawkins position ($P < .01$). There was no significant difference in the proximity of the lesser tuberosity ($P = .69$) and subscapularis insertion ($P = .13$) to the coracoid process for the impingement positions. The radiologic grading of the MR images revealed contact without deformation (grade 1) between the subscapularis and the coracoid process in 1 subject placed in the Neer position and in 3 subjects placed in the Hawkins position.

Internal impingement

The greater tuberosity was significantly closer to the glenoid in the impingement positions than in the neutral position (Figure 4, *B*). Both the infraspinatus and supraspinatus insertions were significantly closer ($P < .01$) to the glenoid in the Neer position than in the Hawkins position (Figures 4, *B*, and 5, *A*). Furthermore, the supraspinatus insertion was significantly closer ($P < .001$) to the glenoid than the infraspinatus insertion for both impingement positions. The distance from the supraspinatus insertion to the glenoid decreased substantially from 35.0 ± 2.8 mm in the neutral position to 18.3 ± 6.2 mm in the Hawkins position and 8.3 ± 2.5 mm in the Neer position.

In both impingement positions, contact of the supraspinatus tendon with the posterosuperior glenoid and labrum was observed in all subjects (Figure 7). Radiologic grading results in the Neer position showed deformation (grade 2) of the supraspinatus muscle-tendon unit by the glenoid and labrum in 5 of 8 subjects. Supraspinatus contact with the labrum without muscle or tendon deformation (grade 1) was observed in the 3 remaining subjects. In the Hawkins position, posterosuperior glenoid impingement with deformation (grade 2) of the supraspinatus was observed in half of the subjects; supraspinatus-labrum contact without deformation (grade 1) was seen in the remaining half of the subjects. The articular surface of the infraspinatus did not make contact with the glenoid rim or labrum (grade 0) in either the Neer or the Hawkins position.

The minimum distance from the lesser tuberosity to the glenoid decreased significantly in the impingement sign positions compared with the neutral position (Figure 4, *B*). Similarly, the subscapularis insertion was significantly closer to the glenoid in the impingement positions than in the neutral position. Both the lesser tuberosity and subscapularis insertion were significantly closer ($P < .05$) to the glenoid in the Hawkins position than in the Neer position. The minimum distance between the subscapularis insertion and glenoid decreased significantly from 19.2 ± 3.0 mm in the neutral position to 5.4 ± 2.5 mm in the Neer position and 3.7 ± 2.0 mm in the Hawkins position (Figures 4, *B*, and 5, *B*).

The radiologic grading of impingement was consistent with the close proximity of the subscapularis

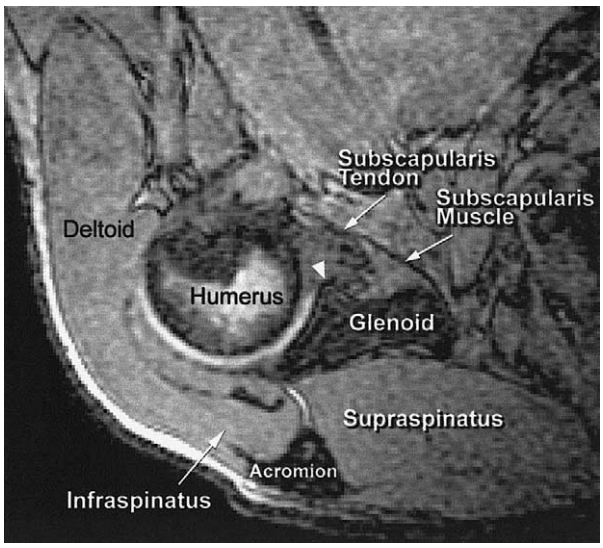

Figure 8 Internal impingement of subscapularis. The image was acquired in the axial plane with subject 3 in the Hawkins position. The subscapularis tendon can be seen making contact with the anterior glenoid and labrum with concomitant deformation (grade 2 impingement).

insertion to the anterior glenoid. Contact without deformation of the subscapularis (grade 1) with the anterior labrum was observed in 7 of 8 subjects when placed in the Neer position. Subscapularis contact with the labrum was seen in all 8 subjects when placed in the Hawkins position; contact of the subscapularis without deformation (grade 1) was observed in 6 of 8 subjects, and deformation of the subscapularis (grade 2) was observed in the 2 remaining subjects (Figure 8).

DISCUSSION

Our study characterized the in vivo anatomy of the Neer and Hawkins impingement sign positions in 8 normal subjects. The Neer position produced statistically significant narrowing of the subacromial space but did not elicit mechanical contact of the rotator cuff tendons with the acromion in any of the normal subjects. This absence of subacromial contact is explained by the posterior and medial location of the greater tuberosity tendon insertion sites relative to the anteroinferior acromion with the arm in the Neer position (Figure 5). In contrast, subacromial contact of either the supraspinatus or the infraspinatus was seen in every subject during the Hawkins maneuver. Although the Hawkins position did not cause significantly greater subacromial narrowing than the Neer position, the Hawkins position did bring the supraspinatus and infraspinatus insertion sites significantly closer to the acromion. In the Hawkins position, the supraspinatus made contact with the medial acromion whereas the infraspinatus made contact with the lateral aspect of the acromion (Figure 7, *B*). Our imaging study also revealed extensive contact of the articular surface of the rotator cuff with the glenoid rim in both the Neer and Hawkins impingement sign positions. For both positions, the supraspinatus insertion was significantly closer to the glenoid than the infraspinatus insertion, which remained more lateral to the glenoid (Figure 5, *A*).

Subacromial impingement

Subacromial contact of the rotator cuff during shoulder abduction and rotation has been characterized by cadaveric studies.[6,7,14] In a study of 9 cadaveric shoulders by Flatow et al,[14] subacromial rotator cuff contact was not observed at 180° elevation but was seen in all shoulders at 90° elevation with 20° internal rotation. Brossmann et al[6] and Burns and Whipple[7] also observed subacromial contact of the supraspinatus in cadaveric shoulders placed in forward flexion and internal rotation. The results of these cadaveric studies are consistent with our observations.

The anatomic relationships within the subacromial space have been studied in vivo by MRI.[23,25,38] Graichen et al[23,25] computed the minimum distance from the humerus to the acromion during abduction and rotation of the shoulder in normal subjects. In all 12 subjects, the minimum acromiohumeral distance vector penetrated the supraspinatus during 90° abduction with 45° internal rotation but passed lateral to the supraspinatus during pure abduction of 120° or greater. This finding is consistent with our observation that in the Neer position, the supraspinatus tendon was medial to the anteroinferior acromion, with its insertion in close proximity to the posterosuperior glenoid (Figure 5, *A*, middle panel).

The anatomy of the Neer and Hawkins maneuvers has been characterized recently by skeletal[12] and cadaveric[40] studies. Edelson and Teitz[12] placed skeletal shoulder specimens in both the Neer and Hawkins sign positions and reported contact between the humerus and acromion only in the Neer position. However, this acromial contact always took place at the surgical neck of the humerus, well beyond the rotator cuff insertion sites. This finding compares well with our surface models of the Neer position, which reveal that the anterolateral acromion was located distal to the tuberosity insertion sites, near the neck of the humerus (Figure 5, middle panels). Valadie et al[40] characterized the anatomy of 9 cadaveric shoulders placed in either the Neer or Hawkins position. In contrast to our study, acromial contact with the greater tuberosity and rotator cuff tendons was more common in the Neer position (5/5 shoulders) than in the Hawkins position (2/4 shoulders).[40] This may be

because of inherent differences between a cadaveric study and an in vivo study.

Using an open MRI scanner, Roberts et al[35] assessed subacromial impingement in 10 asymptomatic volunteers placed in both impingement sign positions. Mechanical contact between the rotator cuff and acromion was not observed in either position. Although this observation differs from our findings, they did measure a significant decrease in the acromiohumeral interval relative to the rotator cuff thickness in the Hawkins position. The methodology of this previous in vivo study differed from ours with regard to subject positioning (seated vs supine), as well as loading conditions (an internal rotation force was not applied in the previous study). In addition, Roberts et al measured distances directly from coronal or sagittal images; a 3D minimum distance analysis was not performed. The presence of internal impingement positions was not assessed by Roberts et al.

Coracoid impingement

Coracoid impingement syndrome is characterized by anterior pain over the coracoid resulting from repeated arm flexion and internal rotation; continuous contact between the coracoid and the lesser tuberosity during this motion is believed to cause damage to the subscapularis tendon.[36] In our study contact of the subscapularis with the coracoid process was observed in 1 subject in the Neer position and in 3 in the Hawkins position. This contact is expected in the Hawkins position, as impingement of the rotator cuff on the coracoid process has been demonstrated during forward flexion to 90° combined with internal rotation.[11,19,20,36] In fact, the coracoid impingement position of cross-arm adduction, forward elevation, and internal rotation[11,13] is very similar to the Hawkins position. Using cine MRI, Friedman et al[15] determined that the coracohumeral interval averaged 11 mm in asymptomatic subjects during maximum internal rotation of the shoulder. This measurement agrees exactly with the mean minimum distance in the Hawkins position measured in our study.

Internal impingement

The concept of internal impingement in the shoulder describes intraarticular contact between the rotator cuff and glenoid rim.[9,31,41] Contact between the articular surface of the supraspinatus and infraspinatus tendons and the posterosuperior glenoid rim with shoulder abduction and external rotation has been demonstrated in arthroscopic,[9,31,41] cadaveric,[28] and MRI[39] studies.

Our study demonstrated a significant reduction in the distance between the greater tuberosity and glenoid in the Neer and Hawkins impingement sign positions, with concomitant contact between the supraspinatus and posterosuperior glenoid in all subjects. Our in vivo observations are consistent with the studies of skeletal specimens by Edelson and Teitz[12] and cadaveric shoulders by Valadie et al.[40] Edelson and Teitz recorded contact between the supraspinatus facet of the greater tuberosity and the glenoid in 26 of 30 shoulder specimens placed in the Neer position and in 25 of 30 specimens placed in the Hawkins position. Valadie et al observed consistent contact between the undersurface of the rotator cuff tendons and the glenoid rim.

In our study the Neer and Hawkins positions brought the lesser tuberosity and subscapularis tendon insertion site into close proximity with the anterior glenoid rim. As a consequence, the deep surface of the subscapularis made contact with the anterior glenoid and labrum in all subjects when placed in the Hawkins position and in all but 1 subject when placed in the Neer position. Cadaveric,[37] imaging,[34,37] and arthroscopic[18] studies have documented that lesions of the subscapularis tendon develop on the deep surface of the tendinous insertion.

Limitations

A potential limitation of our study was the limited number of subjects, all of whom were normal volunteers without shoulder pathology. Additional studies are needed to clarify the anatomic relationships in patients with subacromial impingement syndrome. Subacromial pathology, such as acromioclavicular joint degeneration,[5] and glenohumeral instability[21] can alter anatomic relationships and contribute to subacromial contact and the development of impingement syndrome.[4] Entities such as increased soft-tissue volume in the subacromial space or superior humeral subluxation would be expected to increase the extent of subacromial contact.[14] Differences in acromiohumeral distance[23,24] and subacromial rotator cuff contact[38] have been documented between normal subjects and patients with subacromial impingement syndrome.

The image resolution and slice thickness of our MR images were limited by the total scan time allowed for each shoulder position; the signal-to-noise ratio was limited by the 0.5-T field strength of the open MR scanner. To maximize MR image quality, subjects were imaged in a supine position, rather than a seated position, with the right shoulder near the isocenter of the scanner magnetic field. The resolution of the MR images limited precise mapping of the rotator cuff insertion sites to within approximately 1 to 1.5 mm. Because of the rapid decay of their MR signal, it was difficult to visualize the entire length of ligamentous structures with short T_2 relaxation times such as the coracoacromial, coracohumeral, and glenohumeral ligaments. Additional studies using a high sig-

nal-to-noise ratio and contrast enhancement would be required to further elucidate the in vivo anatomy of structures such as the coracoacromial ligament, which play an important role in subacromial impingement.[6,7,40]

Clinical significance

The results of our study suggest that the Hawkins position elicits substantially greater subacromial contact of the rotator cuff than does the Neer position. Most studies report that subacromial space narrowing and rotator cuff impingement occur most commonly in the middle range of elevation, between 60° and 120°.[14,23,33] Therefore, it is not surprising that the Neer sign position, with the arm in full elevation, would not maximally compress the rotator cuff under the acromion.[14] Our results are also consistent with several studies that found that the combination of forward flexion and internal rotation brings the greater tuberosity into closest proximity to the anteroinferior acromion and maximizes contact of the supraspinatus tendon.[6,7,14,26,35]

Several studies have demonstrated that the Neer and Hawkins signs are sensitive, but poorly specific, clinical tests for diagnosing subacromial impingement syndrome.[8,29,30] Calis et al[8] reported that the Neer and Hawkins signs had a sensitivity of 89% and 92%, respectively, but a specificity of only 31% and 25%, respectively, for subacromial impingement syndrome. Similarly, an arthroscopic study by MacDonald et al[30] reported that the Neer and Hawkins signs had a high sensitivity for subacromial bursitis (75% and 92%, respectively) and for rotator cuff tearing (83% and 88%, respectively). However, the Neer and Hawkins signs were also positive in 25% and 31% of patients with Bankart lesions and 46% and 69% of patients with superior labrum anterior-posterior lesions, respectively.[30]

Our results confirm the findings of recent skeletal[12] and cadaveric[40] studies, which suggest that internal impingement is elicited by the Neer and Hawkins maneuvers, suggesting that intraarticular contact of the rotator cuff with the glenoid occurs physiologically in normal subjects and may play a role in the development of rotator cuff pathology, which often originates on the deep surface of the rotator cuff tendons.[17,22,32]

We gratefully acknowledge the helpful suggestions and assistance of Dr Gordon Campbell.

REFERENCES

1. Arcand MA, Reider B. Shoulder and upper arm. In: Reider B, editor. The orthopaedic physical examination. Philadelphia: Saunders; 1999. p. 19-66.
2. Arnold AS, Salinas S, Asakawa DJ, Delp SL. Accuracy of muscle moment arms estimated from MRI-based musculoskeletal models of the lower extremity. Comput Aided Surg 2000;5:108-19.
3. Besl PJ, McKay ND. A method for registration of 3-D shapes. IEEE Trans Pattern Anal Mach Intell 1992;14:239-56.
4. Bigliani LU, Levine WN. Subacromial impingement syndrome. J Bone Joint Surg Am 1997;79:1854-68.
5. Bigliani LU, Ticker JB, Flatow EL, Soslowsky LJ, Mow VC. The relationship of acromial architecture to rotator cuff disease. Clin Sports Med 1991;10:823-38.
6. Brossmann J, Preidler KW, Pedowitz RA, White LM, Trudell D, Resnick D. Shoulder impingement syndrome: influence of shoulder position on rotator cuff impingement—an anatomic study. AJR Am J Roentgenol 1996;167:1511-5.
7. Burns WC II, Whipple TL. Anatomic relationships in the shoulder impingement syndrome. Clin Orthop 1993;294:96-102.
8. Calis M, Akgun K, Birtane M, Karacan I, Calis H, Tuzun F. Diagnostic values of clinical diagnostic tests in subacromial impingement syndrome. Ann Rheum Dis 2000;59:44-7.
9. Davidson PA, Elattrache NS, Jobe CM, Jobe FW. Rotator cuff and posterior-superior glenoid labrum injury associated with increased glenohumeral motion: a new site of impingement. J Shoulder Elbow Surg 1995;4:384-90.
10. Delp SL, Loan JP. A graphics-based software system to develop and analyze models of musculoskeletal structures. Comput Biol Med 1995;25:21-34.
11. Dines DM, Warren RF, Inglis AE, Pavlov H. The coracoid impingement syndrome. J Bone Joint Surg Br 1990;72:314-6.
12. Edelson G, Teitz C. Internal impingement in the shoulder. J Shoulder Elbow Surg 2000;9:308-15.
13. Ferrick MR. Coracoid impingement. A case report and review of the literature. Am J Sports Med 2000;28:117-9.
14. Flatow EL, Soslowsky LJ, Ticker JB, Pawluk RJ, Hepler M, Ark J, et al. Excursion of the rotator cuff under the acromion. Patterns of subacromial contact. Am J Sports Med 1994;22:779-88.
15. Friedman RJ, Bonutti PM, Genez B. Cine magnetic resonance imaging of the subcoracoid region. Orthopedics 1998;21:545-8.
16. Fung M, Kato S, Barrance PJ, Elias JJ, McFarland EG, Nobuhara K, et al. Scapular and clavicular kinematics during humeral elevation: a study with cadavers. J Shoulder Elbow Surg 2001;10:278-85.
17. Gartsman GM. Arthroscopic management of rotator cuff disease. J Am Acad Orthop Surg 1998;6:259-66.
18. Gerber C, Sebesta A. Impingement of the deep surface of the subscapularis tendon and the reflection pulley on the anterosuperior glenoid rim: a preliminary report. J Shoulder Elbow Surg 2000;9:483-90.
19. Gerber C, Terrier F, Ganz R. The role of the coracoid process in the chronic impingement syndrome. J Bone Joint Surg Br 1985;67:703-8.
20. Gerber C, Terrier F, Zehnder R, Ganz R. The subcoracoid space. An anatomic study. Clin Orthop 1987;215:132-8.
21. Glousman RE. Instability versus impingement syndrome in the throwing athlete. Orthop Clin North Am 1993;24:89-99.
22. Gohlke F, Essigkrug B, Schmitz F. The pattern of the collagen fiber bundles of the capsule of the glenohumeral joint. J Shoulder Elbow Surg 1994;3:111-28.
23. Graichen H, Bonel H, Stammberger T, Englmeier KH, Reiser M, Eckstein F. Subacromial space width changes during abduction and rotation—a 3-D MR imaging study. Surg Radiol Anat 1999;21:59-64.
24. Graichen H, Bonel H, Stammberger T, Haubner M, Rohrer H, Englmeier KH, et al. Three-dimensional analysis of the width of the subacromial space in healthy subjects and patients with impingement syndrome. AJR Am J Roentgenol 1999;172:1081-6.
25. Graichen H, Bonel H, Stammberger T, Heuck A, Englmeier KH, Reiser M, et al. A technique for determining the spatial relationship between the rotator cuff and the subacromial space in arm abduction using MRI and 3D image processing. Magn Reson Med 1998;40:640-3.

26. Hawkins RJ, Kennedy JC. Impingement syndrome in athletes. Am J Sports Med 1980;8:151-8.
27. Jobe CM. Superior glenoid impingement. Current concepts. Clin Orthop 1996;330:98-107.
28. Jobe CM, Sidles J. Evidence for a superior glenoid impingement upon the rotator cuff [abstract]. J Shoulder Elbow Surg 1993;2(Pt 2):S19.
29. Leroux JL, Thomas E, Bonnel F, Blotman F. Diagnostic value of clinical tests for shoulder impingement syndrome. Rev Rhum Engl Ed 1995;62:423-8.
30. MacDonald PB, Clark P, Sutherland K. An analysis of the diagnostic accuracy of the Hawkins and Neer subacromial impingement signs. J Shoulder Elbow Surg 2000;9:299-301.
31. McFarland EG, Hsu CY, Neira C, O'Neil O. Internal impingement of the shoulder: a clinical and arthroscopic analysis. J Shoulder Elbow Surg 1999;8:458-60.
32. Nakajima T, Nobuyuki R, Hamada K, Tomatsu T, Fukuda H. Histologic and biomechanical characteristics of the supraspinatus tendon: reference to rotator cuff tearing. J Shoulder Elbow Surg 1994;3:79-87.
33. Neer CS II. Anterior acromioplasty for the chronic impingement syndrome in the shoulder: a preliminary report. J Bone Joint Surg Am 1972;54:41-50.
34. Pfirrmann CW, Zanetti M, Weishaupt D, Gerber C, Hodler J. Subscapularis tendon tears: detection and grading at MR arthrography. Radiology 1999;213:709-14.
35. Roberts CS, Davila JN, Hushek SG, Tillett ED, Corrigan TM. Magnetic resonance imaging analysis of the subacromial space in the impingement sign positions. J Shoulder Elbow Surg 2002; 11:595-9.
36. Rossi F. Shoulder impingement syndromes. Eur J Radiol 1998; 27(Suppl 1):S42-8.
37. Sakurai G, Ozaki J, Tomita Y, Kondo T, Tamai S. Incomplete tears of the subscapularis tendon associated with tears of the supraspinatus tendon: cadaveric and clinical studies. J Shoulder Elbow Surg 1998;7:510-5.
38. Shibuta H, Tamai K, Tabuchi K. Magnetic resonance imaging of the shoulder in abduction. Clin Orthop 1998;348:107-13.
39. Tirman PF, Bost FW, Garvin GJ, Peterfy CG, Mall JC, Steinbach LS, et al. Posterosuperior glenoid impingement of the shoulder: findings at MR imaging and MR arthrography with arthroscopic correlation. Radiology 1994;193:431-6.
40. Valadie AL III, Jobe CM, Pink MM, Ekman EF, Jobe FW. Anatomy of provocative tests for impingement syndrome of the shoulder. J Shoulder Elbow Surg 2000;9:36-46.
41. Walch G, Boileau P, Noel E, Donell ST. Impingement of the deep surface of the supraspinatus tendon on the posterosuperior glenoid rim: an arthroscopic study. J Shoulder Elbow Surg 1992;1:238-45.